



Astrocytes locally translate transcripts in their peripheral processes

Kristina Sakers^{a,b,c}, Allison M. Lake^{b,c}, Rohan Khazanchi^{b,c}, Rebecca Ouwenga^{a,b,c}, Michael J. Vasek^{b,c}, Adish Dani^{d,e}, and Joseph D. Dougherty^{b,c,e,1}

^aDivision of Biology and Biomedical Sciences, Washington University School of Medicine in St. Louis, St. Louis, MO 63110; ^bDepartment of Genetics, Washington University School of Medicine in St. Louis, St. Louis, MO 63110; ^cDepartment of Psychiatry, Washington University School of Medicine in St. Louis, St. Louis, MO 63110; ^dDepartment of Pathology and Immunology, Washington University School of Medicine in St. Louis, St. Louis, MO 63108; and ^eHope Center for Neurological Disorders, Washington University School of Medicine in St. Louis, St. Louis, MO 63110

Edited by Don W. Cleveland, University of California, San Diego, La Jolla, CA, and approved March 30, 2017 (received for review October 26, 2016)

Local translation in neuronal processes is key to the alteration of synaptic strength necessary for long-term potentiation, learning, and memory. Here, we present evidence that regulated *de novo* protein synthesis occurs within distal, perisynaptic astrocyte processes. Astrocyte ribosomal proteins are found adjacent to synapses *in vivo*, and immunofluorescent detection of peptide elongation in acute slices demonstrates robust translation in distal processes. We have also developed a biochemical approach to define candidate transcripts that are locally translated in astrocyte processes. Computational analyses indicate that astrocyte-localized translation is both sequence-dependent and enriched for particular biological functions, such as fatty acid synthesis, and for pathways consistent with known roles for astrocyte processes, such as GABA and glutamate metabolism. These transcripts also include glial regulators of synaptic refinement, such as *Sparc*. Finally, the transcripts contain a disproportionate amount of a binding motif for the quaking RNA binding protein, a sequence we show can significantly regulate mRNA localization and translation in the astrocytes. Overall, our observations raise the possibility that local production of astrocyte proteins may support microscale alterations of adjacent synapses.

astrocyte | local translation | synapse | TRAP | RNA-sequencing

Astrocytes are required for the proper development and maintenance of the synapse, a structure described as tripartite because of the critical contribution from peripheral processes of these cells (1). There is evidence that astrocytes determine synapse number (2, 3) and strength (4, 5), and reciprocally, that neurons mediate maturation of astrocyte processes (6), yet our mechanistic understanding of these interactions is incomplete.

The localized synthesis of proteins in neurons is instrumental for synaptic modulation (7) and neurite outgrowth (8, 9). Because neurites must extend great distances to reach a target cell, they have the ability to harbor mRNAs and ribosomes proximal to spines and axons (10, 11), where local translation occurs in a precise spatial, temporal, and activity-dependent manner. Similarly, oligodendrocytes also selectively localize some myelin-associated mRNAs for local translation within their ensheathing processes (12). Outside of the nervous system, localized protein synthesis occurs in a variety of biological systems, including *Drosophila* oocytes and migrating fibroblasts, suggesting that this phenomenon is a widely used regulatory system (13, 14).

Peripheral astrocyte processes (PAPs) reach lengths comparable to some neurites, and one astrocyte territory can contact up to 100,000 synapses (15). Furthermore, the dynamic nature of PAPs at synapses requires rapid responsiveness to synaptic changes (5, 16). Therefore, we hypothesized that astrocytes also use local translation. We reasoned that several conditions must be met to establish that local translation occurs in astrocytes: First, both ribosomes and mRNA must be present in PAPs. Second, new protein translation must occur in PAPs. Finally, even if protein synthesis is detected, it is only of substantial interest if it is regulated. Specifically, if local translation in astrocytes exists to support

either local adaptation or specialization of function, as it does in other cells, then it should be biased toward specific transcripts, and these transcripts should contain specific sequence features. Herein, we provide biochemical and imaging evidence for these criteria and define the peripheral translome of the astrocyte.

Astrocyte Ribosomes and mRNA Exist in Their Peripheral Processes, *in Vivo*

Although previous work using electron microscopy (EM) (17) has suggested that ribosome-like structures exist in PAPs, their identity has never been confirmed. We used transgenic mice, where ribosomal protein RPL10A is fused with EGFP specifically within astrocytes (Aldh1L1-EGFP/RPL10A), to localize the large subunit of ribosomes (18). Using *in vivo* immunofluorescence (IF) in cortical astrocytes, we found that EGFP/RPL10A extends beyond GFAP⁺ processes and into peripheral processes surrounded by Aqp4, which marks astrocyte membranes and vascular endfeet (19) (Fig. S1 A and B). We then asked if we could detect tagged ribosomes in perisynaptic PAPs using both immuno-EM and a recently developed approach leveraging stochastic optical reconstruction microscopy (STORM), allowing for ultrastructural-level resolution compatible with multicolor fluorescent labeling (20).

Significance

Cellular compartments are specialized for particular functions. In astrocytes, the peripheral, perisynaptic processes contain proteins specialized for reuptake of neurotransmitters and ions, and have been shown to alter their morphology in response to activity. Regulated transport of a specific subset of nuclear-derived mRNAs to specific compartments is thought to support the specialization of these compartments and allow for local regulation of translation. In neurons, local translation near activated synapses is thought to generate the proteins needed for the synaptic alterations that constitute memory. We demonstrate that astrocytes also have sequence-dependent local translation in their peripheral processes, including transcripts with roles in regulating synapses, and identify one mechanism regulating this translation. These findings suggest local translation in astrocyte processes may play a role in synapse modulation.

Author contributions: K.S., A.D., and J.D.D. designed research; K.S., R.K., and A.D. performed research; R.O., M.J.V., and A.D. contributed new reagents/analytic tools; K.S. and A.M.L. analyzed data; and K.S. and J.D.D. wrote the paper.

Conflict of interest statement: J.D.D. has received royalties for the translating ribosome affinity purification (TRAP) method.

This article is a PNAS Direct Submission.

Data deposition: The data reported in this paper have been deposited in the Gene Expression Omnibus (GEO) database, <https://www.ncbi.nlm.nih.gov/geo> (accession no. GSE74456).

¹To whom correspondence should be addressed. Email: jdougherty@genetics.wustl.edu.

This article contains supporting information online at www.pnas.org/lookup/suppl/doi:10.1073/pnas.1617782114/-DCSupplemental.

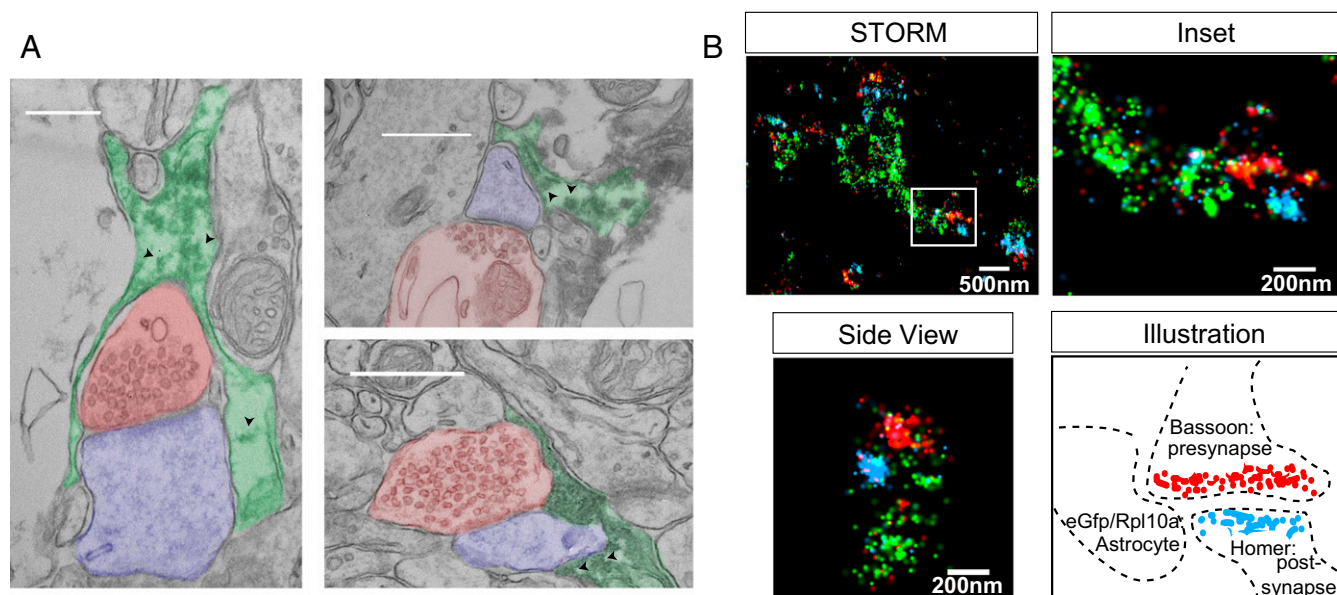


Fig. 1. EM and STORM show astrocyte ribosomes in close proximity to synapses, in vivo. (A) Representative electron micrographs of DAB-labeled EGFP/RPL10A (arrowheads) in astrocyte processes (green) near cortical synapses (axon = blue and postsynaptic density = red). (Scale bars, 500 nm.) (B) STORM imaging showing an EGFP/RPL10A (green) filled astrocyte process proximal to synapses [as illustrated, these are defined by apposition of Bassoon (red) and Homer (blue)]. Inset of box on Left, and side view is a 90° rotation of a second synapses, again showing EGFP/RPL10A puncta surrounding a synapse.

Astrocyte EGFP/RPL10A was found surrounding synapses via EM (Fig. 1A) and within 100 nm of synapses, which are defined by apposition of pre- and postsynaptic markers via STORM (Fig. 1B). Because translation requires both large and small subunits, we confirmed peripheral localization of endogenous small ribosomal subunits via RPS16 IF (Fig. S1C), indicating the tagged RPL10A is not mislocalized in the Aldh1L1-EGFP/RPL10A mice. Together, these data provide strong evidence that astrocyte ribosomes are present near cortical synapses.

We next sought to confirm the presence of mRNA within PAPs. We chose to focus on the localization of *Slc1a2* (GLT-1) for two reasons: first, GLT-1 protein is highly expressed in PAPs (21) and second, previous colorimetric in situ hybridization suggested its peripheral localization (22). Because conventional immunolabeling methods did not allow us to distinguish the peripheral processes of neighboring astrocytes from one another, we developed a viral method to sparsely GFP-label astrocytes in nontransgenic mice (Fig. S2). Using this approach, we confirmed that *Slc1a2* mRNA is found throughout the astrocyte, including in distal GFAP⁺ PAPs (Fig. S1D).

Astrocyte Processes Synthesize Proteins in Their Distal Tips

After demonstrating the presence of both ribosomes and mRNA in PAPs, we next tested whether distal translation occurs by using puromycin to label actively translating peptides in acute brain slices (Fig. 2A). Puromycin, a tRNA-structural analog, incorporates into translating ribosomes and puromycylates the growing peptide (23). Using an antibody against puromycin for IF in sparsely labeled astrocytes (Fig. 2A and Fig. S3A), we detected nascent translation within PAPs, which was blocked by pretreatment with the translation inhibitor, anisomycin, indicating that puromycin labeling requires active translation (Fig. 2B). We quantified the total translation occurring throughout the astrocyte by measuring the fluorescence intensity of puromycin within GFP and puromycin double-positive puncta at increasing radii from the nucleus of the astrocyte. We empirically determined that a 27- μ m radius captures the majority of the astrocyte, without extending into neighboring astrocyte territories (Fig. S3B), consistent with previous data describing a mean murine astrocyte diameter of 56 μ m (15). Given the short duration

of incubation, we concluded that puromycylated peptides in PAPs were made locally rather than transported. Quantification of puromycylation in astrocytes indicates that on average 73% of translation in an astrocyte occurs >9 μ m from the nucleus center (Fig. 2C), and does not taper significantly as it extends to the periphery.

PAP-Translating Ribosome Affinity Purification Reveals Hundreds of Enriched Ribosome-Bound Transcripts in PAPs

In neurons, local translation appears to be enriched for certain transcripts, often those generating proteins with synaptic roles. If translation in PAPs does indeed have a physiological role, then a specific subset of astrocyte transcripts should show enriched translation there. We hypothesized that local translation is sequence-dependent, and furthermore will be enriched for transcripts consistent with the known roles of the PAP (e.g., glutamate homeostasis).

To test this hypothesis, we developed a method to capture ribosome-bound mRNA from PAPs using translating ribosome affinity purification (PAP-TRAP) (Fig. 3A). Synaptoneurosomes (SNs) are translation-competent membrane-enclosed appositions of pre- and postsynaptic specializations that can be purified from brain homogenates by density fractionation. Although the neuronal contents of SN fractions have been well-described, a preliminary RNA-sequencing of the total SN fraction suggested substantial contribution of mRNAs from nonneuronal cells. This finding is in agreement with a prior RT-PCR observation of an astrocyte transcript in SNs (24). Furthermore, immunoblot confirmed SN fractions contain Ezrin, a constituent of PAPs (25), and astrocytic EGFP/RPL10A, as well as the expected enrichment of PSD95 and depletion of nuclear Lamin B2 (Fig. 3B). Therefore, to define the RNAs being translated by astrocytes in the SN, we isolated astrocyte-tagged ribosome-bound RNA from the fraction (Fig. S4), and performed RNA-seq on the PAP-TRAP sample and three-comparison samples (Dataset S1).

We next leveraged these data to identify those transcripts with enriched ribosome occupancy in the PAP. Because all RNAs must move from the nucleus through the soma to arrive in PAPs, we did not expect to find transcripts that are only found in PAPs and not in the soma. Rather, we used an intersection of two comparisons

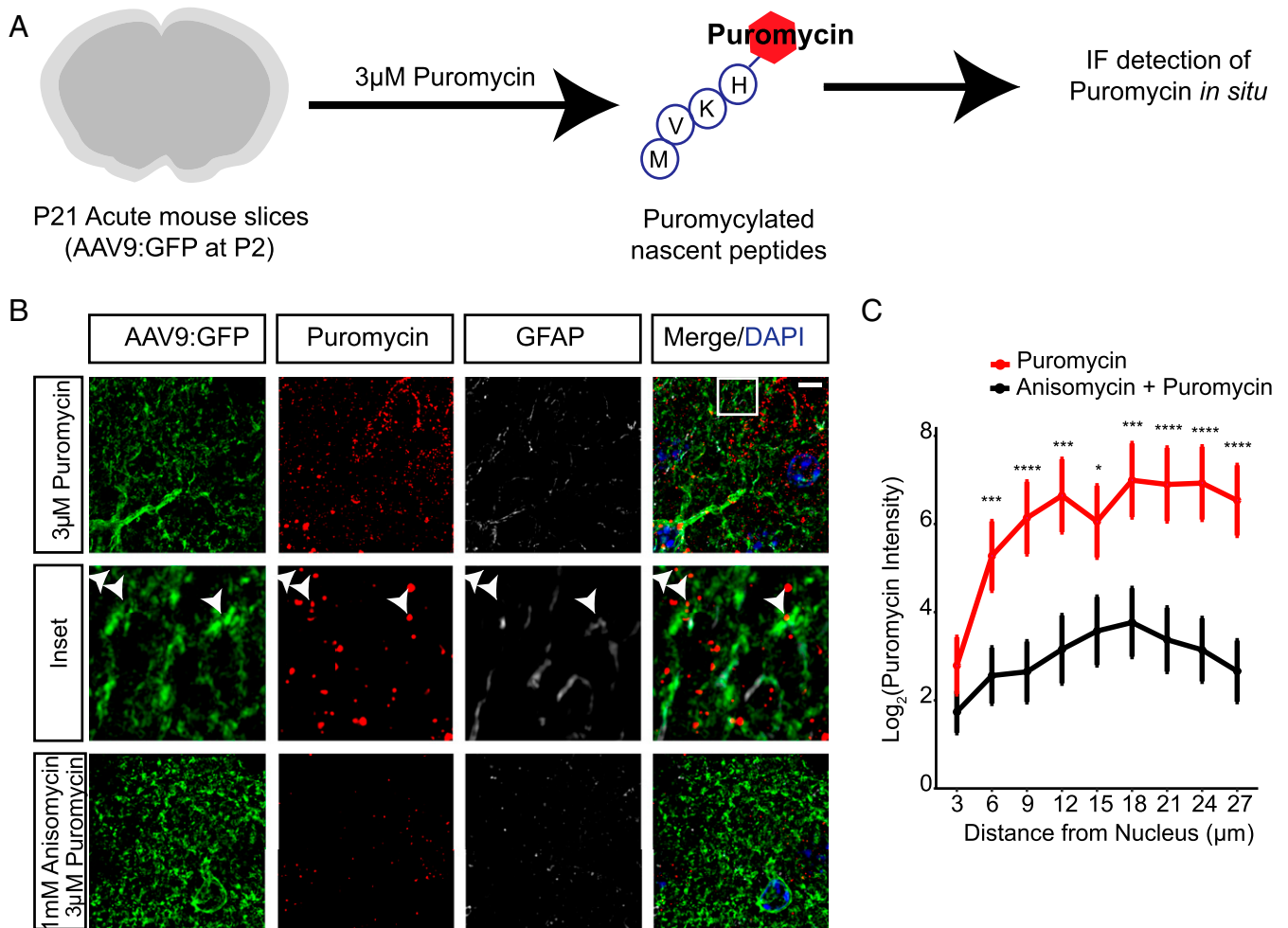


Fig. 2. Peripheral ribosomes are actively translating in astrocytes. (A) Cartoon diagram of puromycylation experiments. Acute slices (cartooned in gray) are incubated with puromycin (red hexagon) which attaches to the growing peptide (cartooned by amino acid abbreviations in circles). Slices are then prepared for IF detection of puromycin. (B) Maximum projection superresolution SIM to detect puromycylation (red) of synthesizing proteins in a GFP-labeled astrocyte shows translation occurs in peripheral processes, and is blocked by pretreatment with anisomycin. Arrowheads indicate puromycylated peptides colocalized with GFP-positive peripheral astrocyte processes. (Scale bar, 10 μm .) (Magnification, 100 \times .) (C) Quantification of puromycin intensity (only puromycin pixels that were in astrocytes labeled with GFP were measured) at increasing radii from the nucleus indicates robust translation occurs in PAPs. Repeated-measures ANOVA revealed main effects of condition $F_{(2, 138)} = 9.694$, $P = 0.0001$ and distance $F_{(8, 1,104)} = 19.023$, $P < 2\text{E-}16$ with a significant interaction between condition and distance $F_{(16, 1,104)} = 2.019$, $P = 0.01$. Data represented as mean \pm SEM. Asterisks represent one-sided t tests, post hoc. **** $P < 0.001$, *** $P < 0.005$, * $P < 0.05$. n (cells) = 54 (puromycin), 48 (anisomycin+puromycin).

to derive a stringent list of PAP translated candidates. First, we compared SN RNA-seq to cortex-input RNA-seq to enrich for transcripts localized to the fraction. This, by itself, would identify putatively localized transcripts, but would contain transcripts from many cell types. Thus, we intersected this set with those transcripts enriched on astrocyte ribosomes in the SN (PAP-TRAP/SN). This combined analysis identified 224 transcripts that are significantly enriched on PAP ribosomes (Fig. 3 C–E and Dataset S2), including *Slc1a2*.

We also tested a direct statistical comparison of PAP-TRAP to TRAP samples as an alternative method of defining locally translated astrocyte transcripts. Whereas the resulting analysis included all 224 discovered transcripts above, it also included several clearly spurious transcripts (e.g., mitochondrial transcripts not translated on the eukaryotic ribosome) that are most clearly attributable to a difference in background levels of contaminating RNA between TRAP and PAP-TRAP. We found that although PAP-TRAP still enriches for known astrocyte transcripts relative to SN samples, there is a blunting of both enrichment of known astrocyte markers and depletion of neuronal markers relative to a

control cortex TRAP (Fig. 3 C and D). Although we are interested in further optimizing PAP-TRAP to reduce this background, and thus increase sensitivity to define additional transcripts, our current intersectional analysis appears robust. The analysis includes several canonical astrocyte markers (Fig. 3F), and overlaps with both mRNA detected in astrocyte processes in vitro (26) and those just reported for radial glia in vivo (27) (Fig. S54). Thus, we proceeded with analysis of the 224 high-confidence transcripts.

For computational analyses, we also generated a contrasting set of transcripts depleted from the PAP using a reciprocal approach: we intersected the transcripts depleted from the SN relative to cortex input, but still enriched on astrocytes ribosomes by TRAP. We identified 116 astrocyte transcripts (“PAP-depleted” transcripts) (Fig. 3E and Dataset S3).

PAP-Enriched Transcripts Suggest Physiological Roles for Local Translation, Including Modulation of Neurotransmitter Metabolism

To provide a systems perspective as to functions local translation might serve in astrocytes, we performed pathway analyses on the

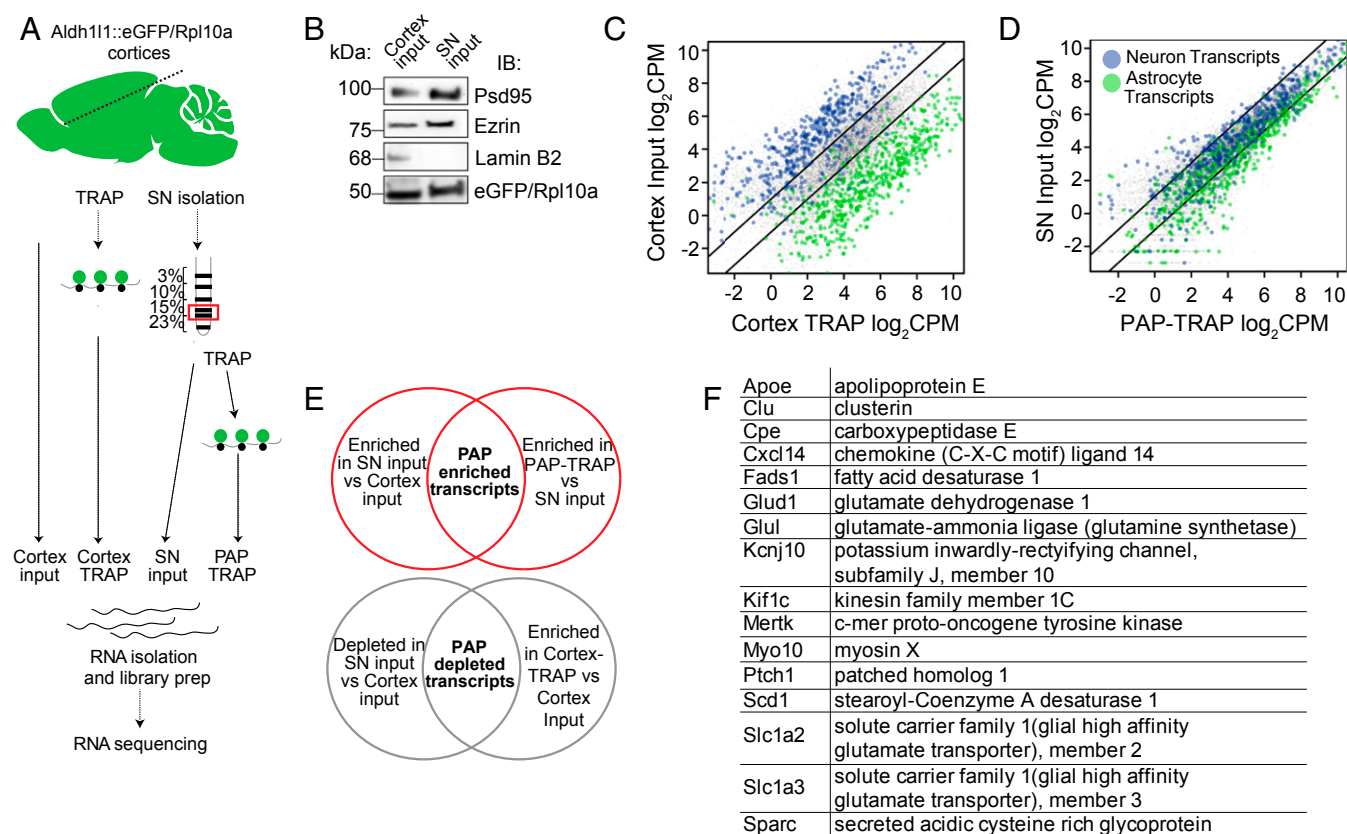


Fig. 3. Identification of peripherally enriched transcripts. (A) Diagram of experimental steps in PAP-TRAP and comparison samples for RNA-seq. (B) Representative immunoblots for input and SN fraction confirms enrichment of synaptic and PAP proteins, depletion of nuclear proteins (LaminB2), and presence of EGFP/RPL10A. (C and D) cpm plots of astrocyte and neuron transcripts after TRAP from the cortex (C) or from the SN fraction (D). Lines denote twofold enrichment/depletion. We detect robust enrichment for sets of ~200 previously detected (60) astrocyte-enriched transcripts (green dots), and substantial, although not complete, depletion of ~200 previously detected (60) neuron-enriched transcripts (blue dots) in the current cortex-TRAP experiment. This degree of enrichment and depletion is typical for TRAP (61, 62). (E) Diagram of analytical strategy for defining PAP-enriched/depleted transcripts. (F) Examples of PAP-enriched transcripts, including those related to glutamate metabolism (*Slc1a2*, *Slc1a3*, *Glul*), fatty acid synthesis (*Fads*, *Scd*), and interesting signaling molecules (*Ptch1*, *Sparc*, *Ntsr2*).

PAP-enriched transcripts (Fig. 4A and Fig. S6A). We found that PAP-localized transcripts had overrepresentation of genes mediating glutamate and GABA metabolism, consistent with PAP functions of glutamate transport (*Slc1a2*, *Slc1a3*) (21, 28) and metabolism (*Glul*). We also identified a set of enzymes representing multiple steps in a pathway for biosynthesis of unsaturated fatty acids (*Scd1*, *Scd2*, *Fads1*, *Fads2*, *Elovl5*, *Hadha*), suggesting a novel hypothesis that there may be some local regulation of fatty acid production either for signaling or expansion of local membrane. We also identified several motor and cytoskeletal proteins (e.g., *Kif1c*, *Myo1D*), local translation of which could play a role in morphological remodeling of astrocyte processes. Finally, we also noticed an enrichment for genes and members of gene families known to regulate synapse number (*Mertk*, *Sparc*, *Thbs4*) (29–31), suggesting that synapse formation and elimination may be mediated in part by local translation of cues from adjacent astrocytes. In contrast, PAP-depleted transcripts have largely nonoverlapping Gene Ontology (GO) categories with PAP-enriched transcripts, and are enriched for transcription regulators and amino acid catabolism (Fig. S6B).

PAP-Enriched Transcripts Have Longer 3'UTRs and Are More Highly Expressed than PAP-Depleted Transcripts

For some well-characterized dendritically localized transcripts, as well as the localization of *Actb* in fibroblasts, sequence-specific features are commonly found within the 3'UTR that mediate

their localization (32–34) or localized translation. Therefore, we tested whether PAP-enriched transcripts contain sequence-specific features. We found no differences in individual nucleotide or GC content (Fig. S7). However, PAP-enriched transcripts were expressed significantly higher in cortical astrocytes compared with PAP-depleted transcripts (Fig. 4B). In neurons, locally translated mRNAs, often sequestered by RNA-binding proteins (RBPs) into granules for transport and protection, have significantly longer 3'UTRs (35). This aspect may enable more sequence motifs or secondary structure for binding RBPs. We found that PAP-enriched transcripts are also significantly longer, specifically in their 3'UTRs (Fig. 4C). Because RBPs may recognize secondary structure rather than specific sequence, we used the RNA-folding algorithm, ViennaRNA (36), to investigate the stability of transcript 3'UTRs in the PAP-enriched/depleted transcripts. Interestingly, we found that PAP-enriched 3'UTRs are predicted to have more stable secondary structures (Fig. 4D). The greater length and structure suggests that sequences in 3' UTRs may also serve to regulate the localized enrichment of specific mRNAs in PAPs, perhaps because of the presence of specific motifs.

Evidence for Multiple Mechanisms of Regulation of Localized Translation

There are at least two mutually nonexclusive mechanisms by which particular transcripts could show increased translation at the PAP. First, the mRNAs could have motifs that enrich their

and the half site may lie upstream or downstream of the core. Thus, to confirm the results from AME, we independently searched for the complete motif and found that a significantly higher percentage of PAP transcripts contain a QRE, compared with PAP-depleted transcripts (Fig. 6A). Interestingly, Qk has a known role in mRNA export from the nucleus. In oligodendrocytes of Qk viable mice, myelin basic protein mRNA is restricted to the nucleus and thus cannot be locally synthesized, inevitably causing dysmyelination and a quaking phenotype (41, 42). Therefore, we hypothesized that QREs may play a role in local translation of PAP transcripts. Qk is present in astrocytes and is known to regulate *Gfap* in primary human astrocytes (43, 44). Here, we chose to focus on the *Sparc* 3'UTR that has two putative QREs (Fig. 6B), is secreted from astrocytes, and has been shown to specifically antagonize the synaptogenic effects of the protein Hevin, thus suggesting a physiological role for local translation (30, 45). We first asked whether *Sparc* is bound by Qk in vivo by immunoprecipitation (IP) the three Qk isoforms, QKI-5, -6, and -7 (Fig. 6C). We found that *Sparc* co-IPs with the nuclear isoform, QKI-5 and one cytoplasmic isoform, QKI-6, but not QKI-7 (Fig. 6D).

To directly probe whether RNA localization is altered with the loss of the QREs, we designed astrocyte-specific viral reporter constructs in which a membrane-bound cerulean fluorescent protein (mCFP) is followed by the *Sparc* 3'UTR, with or without both QREs (Fig. 6E and Fig. S2), under the control of a GFAP promoter to sparsely label astrocytes as above. Quantification of total FISH intensity in each cell was not different between conditions (Fig. 6F); however, we did notice an increase in nuclear localized CFP mRNA intensity (Fig. 6G) when we deleted the QREs from *Sparc*, in a subset of the astrocytes. When we quantified the number of cells in each condition with nuclear RNA foci, we found that significantly more cells contained nuclear RNA when we deleted *Sparc*'s QREs (Fig. 6H). We confirmed this is not the result of an artifactual hybridization to viral episomal DNA because a nuclear RNA remained after treatment with RNase H. Additionally, we noticed that CFP protein appeared consistently brighter in cells that were transduced with *Sparc* 3'UTR without the QREs. We quantified the IF signal intensity of cells in each condition and found that cells transduced with *Sparc* 3'UTR without QREs had significantly more CFP protein (Fig. 6I). Finally, to determine whether these aspects of QRE function will result in a different subcellular distribution of the translated protein, we examined distribution of mCFP after normalizing for expression levels. We found QREs altered the relative concentration of mCFP in the distal compartments (Fig. 6J). Overall, these data indicate that the QREs promote nuclear export of *Sparc* and, without affecting RNA abundance, also serve to suppress translation and shift the relative proportion of proteins.

Discussion

Here we present evidence of localized translation of specific transcripts in astrocytes. We have provided evidence that ribosomes and mRNA are localized throughout the astrocyte, and by labeling of new protein synthesis with a brief pulse with puromycin have confirmed new peptide synthesis throughout the cell. We also use a biochemical method to enrich for ribosome-bound transcripts in PAPs. Our data indicate that these PAP-enriched candidates have a median higher expression and a significantly longer and more stable 3'UTR than those transcripts not enriched in the PAP. The higher median expression suggests one mechanism that prevents distal translation for some transcripts might be destabilizing elements that lead to a short half-life, and indeed many proteins with roles in transcription regulation have such elements (46). The 3'UTR length and structure differences suggest that localization information exists in the 3'UTR, as is the case with many dendritically translated transcripts (33). As proof of this concept, we found that the QRE is enriched in PAP transcripts

and in the context of the *Sparc* 3'UTR, promotes nuclear export and decreases translational efficiency. Although we did not find a difference in peripherally localized RNA in the absence of QREs, mRNA export is a key first step in localization and may contribute to a multistep mechanism of peripheral localization. Additionally, it is thought that translational repression of locally translated mRNAs is a critical step in proper spatial expression of the protein (47, 48). Thus, Qk may bind PAP-localized mRNAs and suppress translation during transport or to keep the mRNA in a poised state at the PAP until receipt of an unknown cue. When tested with a reporter gene, the consequence of removing the QREs was to increase the relative protein abundance in the periphery, consistent with other motifs in the RNA regulating peripheralization of the mRNA, whereas the QRE suppresses translation. Understanding of additional mechanisms governing astrocyte local translation will provide insight to the phenomenon and opportunities to test the physiological relevance.

We also demonstrate the complexity of mRNA localization in astrocytes, in vivo, with FISH. These data motivate the development of tools for labeling PAPs, as we demonstrated that mRNA localization does not follow simple patterns based on distance from the nucleus. We hypothesize that the subcellular domains in astrocytes may rather be specified by their proximity to CNS structures, such as synapses and blood vessels, and this likely contributes to the variability in mRNA distribution within and across probes when using our current proxy measure (Fig. 5). Finding RNA or protein markers of any such domains would advance the field, as would application of methods like merFISH (49), to determine which mRNA species are coenriched in particular puncta within an astrocyte.

Interestingly, we detected a few neuron-derived transcripts copurifying and enriched with SN-localized astrocyte ribosomes (Dataset S2), but we conclude that the removal of these transcripts from the data does not change the overall conclusions presented herein (Fig. S5 and Dataset S4). However, the possible mechanisms for this signal may reveal interesting biology and are of interest for future study.

We note that our current list of locally translated candidates includes several disease genes; most notably, the Alzheimer's-associated gene *ApoE* appears to be robustly enriched in the PAP. Furthermore, at least two dysregulated transcripts identified via TRAP in astrocytes in amyotrophic lateral sclerosis (ALS) models (*Hevl* and *Vim*) (50), as well as *Slc1a2*, which is downregulated in the motor cortex of ALS patients (51), are enriched in the PAP. It is possible that dysregulation of local translation may contribute to disease progression and vulnerability of adjacent neurons. The PAP-TRAP method should be readily adaptable to study such possibilities in mouse models of neurological disorders.

Whereas local translation in neurons has been described for decades, only a few studies have been able to address its physiological role. Although we do not yet have the tools to directly probe the physiological role of peripheral astrocyte translation, our pathway analyses provide interesting clues. We found that the transcripts for secreted protein precursors are found in PAPs (*Clu*, *Cpe*, and *Sparc*), all of which have been identified as enriched in astrocyte-conditioned media by mass spectrometry (45). This finding suggests that these glial-derived soluble signaling molecules are locally synthesized before their extracellular release. Furthermore, we noted several peripherally enriched transcripts for proteins with known roles in synapse maintenance, including *Sparc*, and *Mertk*. It has been shown that *Sparc* negatively regulates excitatory synaptogenesis by antagonizing Hevin (30). Furthermore, *Mertk* is a required engulfment receptor for astrocyte-mediated synapse elimination, in vitro and in vivo (29). Together, these findings provide evidence consistent with the exciting possibility that localized translation might have a role in a localized astrocyte-mediated synaptic modulation. Overall our data indicate

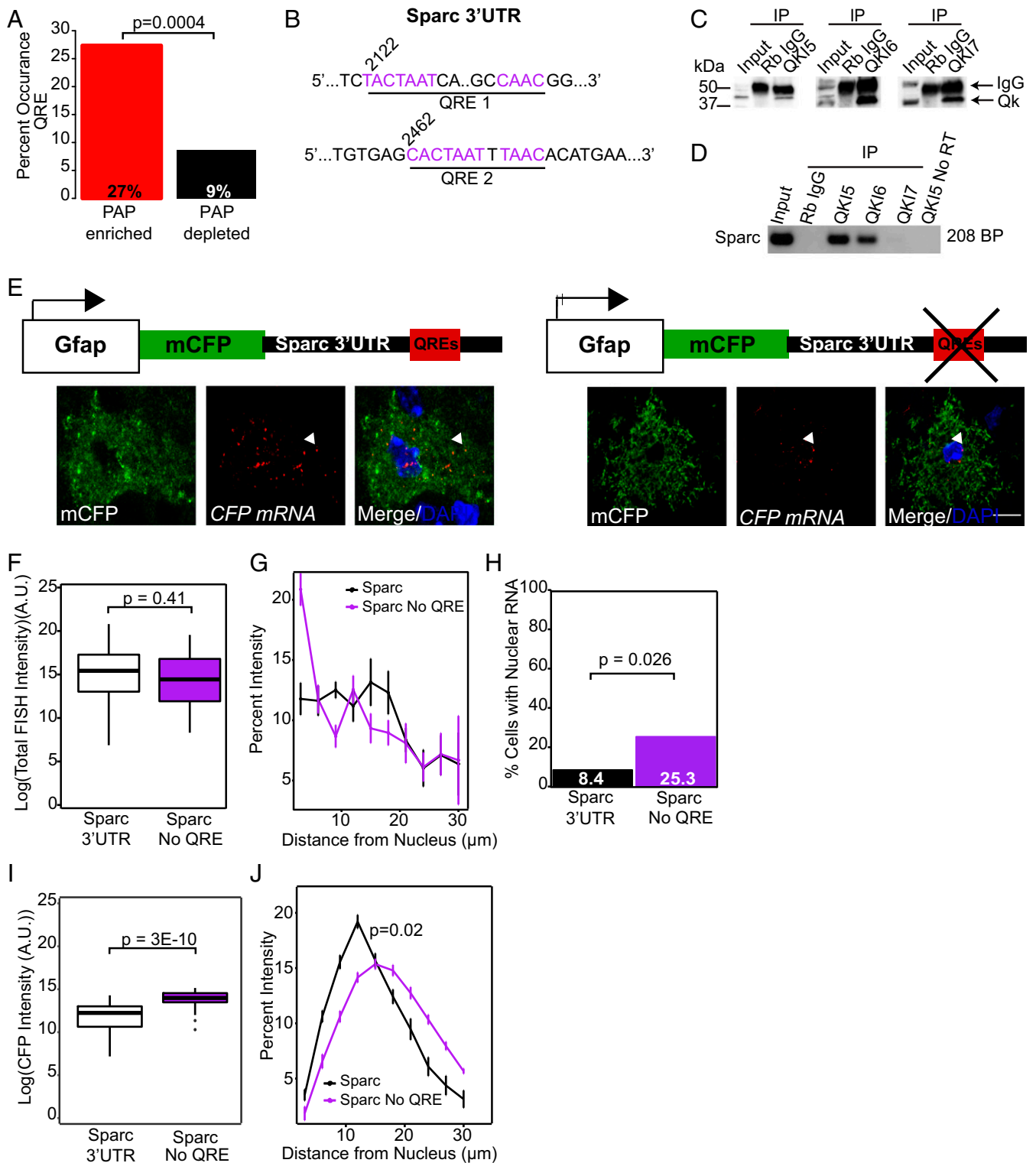


Fig. 6. Qk promotes nuclear export of *Sparc* mRNA and controls its translational efficiency. (A) Percent of transcripts in PAP-enriched/depleted lists that contain the QRE core and half sites NACUAAY-N_(1,20)-YAAY, one-tailed Fisher's exact test. (B) Sparc 3'UTR cDNA sequences that contain putative QREs, numbers indicate position (NM_001290817). (C) Qk isoforms 5, 6, and 7 were immunoprecipitated from adult mouse brain and isolated material was analyzed on a Western blot with Qk antibodies. Total mouse IgG was used in negative IP controls. (D) RT-PCR of *Sparc* after isolation of Qk or mouse IgG-bound RNA. (E) Cartoon schematic of viral constructs with representative confocal images from each condition. Arrows indicate representative examples of RNA localized in the periphery (Sparc 3'UTR) vs. soma/nucleus (Sparc no QRE) of the cell. (Scale bar, 10 μm .) (F) Boxplots of FISH intensity throughout the entire cell, student's two-tailed *t* test. (G) Percent intensity of FISH signal across distance, normalized within cell. Repeated-measures ANOVA main effect of distance: $F_{(1, 1,240)} = 47.132$, $P = 1.05E-11$. (H) Number of cells containing nuclear RNA foci, one-tailed Fisher's exact test. (I) CFP protein intensity in each cell, Wilcoxon rank-sum test. (F–H) $n = 67$ (Sparc), 71 (Sparc no QRE); (I) $n = 53$ (Sparc), 46 (Sparc no QRE). (J) Percent intensity of CFP protein across distance, normalized within cell. Repeated-measures ANOVA main effects of condition $F_{(1, 97)} = 6.025$, $P = 0.0159$ and distance $F_{(1, 97)} = 11.21$, $P = 0.0012$ and a significant interaction between them $F_{(1, 97)} = 30.08$, $P = 3.29E-7$.

that astrocytes are capable of a sequence-regulated localized translation. We posit here that, whereas neurons are thought to require localized translation to compensate for the great length of their dendrites and axons, astrocytes contacting multiple synapses may use local translation to allow for them to respond to or modulate the activity of specific synapses.

Materials and Methods

Animals. All procedures were approved by the Institutional Animal Care and Use Committee at Washington University in St. Louis.

Viral Delivery. AAV9 GFAP-mCherry or AAV9 CBA-IRES-GFP and was delivered by intracranial injections in postnatal day (P)2 pups, and tissues were harvested at P21.

Acute Slice Preparation and Drug Treatment. Acute cortical slices (300 μ m) were prepared as described previously (52). Slices were incubated with 3 μ M puromycin (Tocris #40–895-0) for 10 min at 37 °C. In controls, 1 mM anisomycin (Sigma #A9789) was added to slices 30 min before puromycin.

IF. For IF, 40- μ m sections were cryosectioned after 4% paraformaldehyde (PFA) perfusions. Sections were incubated with primary antibodies (Table S1) followed by Alexa-conjugated secondary antibodies (Invitrogen) and DAPI. For STORM, Jackson ImmunoResearch secondary antibodies were conjugated with acceptor (Cy2, Cy3, or Alexa 405) and reporter (Alexa 647) fluorophore dye pairs and imaged as described previously (53). Representative images are from triplicate experiments.

FISH. FISH was performed on 14- μ m slide-mounted cryosections after 4% PFA fixation of virally injected animals. Custom digoxigenin-labeled antisense probes were hybridized overnight, washed, H₂O₂-blocked, Dig-antibody-labeled, and detected via Tyramide Signal Amplification Cyanine 3 Tyramide (PerkinElmer #NEL704A001KT) as described previously (54). IF was subsequently performed. See Table S2 for primers for FISH probe templates.

Microscopy. Confocal microscopy used an UltraVIEW VoX spinning disk (PerkinElmer) or an AxioImager Z2 (Zeiss). Structured illumination microscopy (SIM) microscopy was performed on a Nikon n-SIM. STORM images were acquired on a custom-built microscope.

Quantification. We drew concentric rings around the nucleus with increasing radii of 3 μ m, in ImageJ, and quantified intensity of CFP; the extent of FISH or puromycin intensity and area overlapping with GFP/CFP were quantified for each ring.

EM. Mice were perfused with 37 °C Ringer's solution, then 37 °C 4% PFA, then postfixed. Next, 100- μ m coronal vibratome sections were cut, rinsed, H₂O₂-blocked, washed, incubated in 1% sodium borohydride, washed then incubated with anti-GFP, then Vectastain ABC elite (Vector Laboratories, PK-6100), and washed in 0.1 M sodium acetate, then labeled with nickel-enhanced DAB before postfixation. Samples were then prepared for EM, as described previously (55). The 70-nm-thin sections were imaged on a JEOL JEM-1400 Plus at 80 KeV.

IP. Qk was immunoprecipitated by coupling QKI antibody to Biotinylated-Protein G (Pierce) on Streptavidin M280 Dynabeads (Invitrogen). C57bl6/j brains were homogenized, lysed, and incubated with beads at 4 °C. Beads were washed and split for RNA isolation (75%) and Western blotting (25%).

SN Preparation. Three cortices (including hippocampi) per replicate were homogenized from Aldh111:EGFP/RPL10A mice and homogenate was spun at 1,000 \times g for 10 min at 4 °C, layered onto a sucrose-Percoll gradient as described previously (56), and spun at 32,500 \times g for 5 min. The SN band was collected by puncturing the bottom of the tube to collect the SN fractions.

Western Blots. For three independent replicates, lysates were separated on 4–12% polyacrylamide gel (Bio-Rad), transferred to PVDF, and probed with primary antibodies (Table S1) and HRP-coupled secondaries (Bio-Rad).

TRAP-seq. TRAP was performed on three replicates of SN fraction (PAP-TRAP sample) and cortex homogenate (cortex-TRAP sample), modified from protocols as described previously (18, 57). RNA quality and concentration were assessed using PicoChips on the Agilent BioAnalyzer (Fig. S4). Double-stranded cDNA was prepared using the Nugen Ovation RNA-seq System V2. Illumina sequencing libraries using the NEBNext Ultra DNA Library Prep Kit for Illumina (#E73705). Libraries were sequenced on an Illumina HiSeq. 2500, for a total of 195 M 50-bp reads across the 12 samples. Reads were analyzed as described previously (54). Raw and analyzed RNA-sequencing data are also available at the Gene Expression Omnibus, accession no. GSE74456.

GO Analysis. PAP-enriched and -depleted lists (Fig. 3E) were analyzed using the BiNGO plugin (v3.0.3) in Cytoscape (v3.2.1). Mouse genome informatics IDs and descriptions were obtained from the biomaRt package from Bioconductor in R. Overrepresented biological processes were identified using a hypergeometric test with Benjamini-Hochberg. Lists were compared with a background list of genes detected at counts per million (cpm) > 2 in the cortex-input sample.

Sequence Features. For each gene, the sequence of the longest isoform was used. All comparisons between lists were made with Wilcoxon rank-sum test with Benjamini-Hochberg correction. For RNA structure, we used the ViennaRNA RNAfold (58) program, and normalized for length. AME used the MEME-suite (59) webtool on PAP-enriched transcripts, using PAP-depleted transcripts as control sequences, with default parameters and Fisher's exact test. The QRE (40) motif was independently validated with a custom R script.

ACKNOWLEDGMENTS. We thank Dr. Joshua Dearborn, Dr. Min-Yu Sun, Dr. Dennis Oakley, Dr. Matt Joens, and Dr. James Fitzpatrick for training and support; Dr. Kelly Monk, Kayla Nygaard, and Bernard Mulvey for comments; and members of the J.D.D. laboratory for advice. This work was supported by the Children's Discovery Institute (CDI) (MD-II-2013-269), the NIH (DA038458-01, MH099798-01, NS086741, 5T32 GM081739, T32 GM008151), and a CDI microgrant (CDI-CORE-2015-505), the Foundation for Barnes-Jewish Hospital (3770), the Hope Center by the Viral Vectors Core, and the Genome Technology Resource Center at Washington University in St. Louis (NIH P30CA91842 and UL1TR000448).

- Araque A, Parpura V, Sanzgiri RP, Haydon PG (1999) Tripartite synapses: Glia, the unacknowledged partner. *Trends Neurosci* 22:208–215.
- Ullian EM, Sapperstein SK, Christopherson KS, Barres BA (2001) Control of synapse number by glia. *Science* 291:657–661.
- Mauch DH, et al. (2001) CNS synaptogenesis promoted by glia-derived cholesterol. *Science* 294:1354–1357.
- Pfrieger FW, Barres BA (1997) Synaptic efficacy enhanced by glial cells in vitro. *Science* 277:1684–1687.
- Jourdain P, et al. (2007) Glutamate exocytosis from astrocytes controls synaptic strength. *Nat Neurosci* 10:331–339.
- Swanson RA, et al. (1997) Neuronal regulation of glutamate transporter subtype expression in astrocytes. *J Neurosci* 17:932–940.
- Kang H, Schuman EM (1996) A requirement for local protein synthesis in neurotrophin-induced hippocampal synaptic plasticity. *Science* 273:1402–1406.
- Kislauskis EH, Li Z, Singer RH, Taneja KL (1993) Isoform-specific 3'-untranslated sequences sort alpha-cardiac and beta-cytoplasmic actin messenger RNAs to different cytoplasmic compartments. *J Cell Biol* 123:165–172.
- Zhang HL, et al. (2001) Neurotrophin-induced transport of a beta-actin mRNA complex increases beta-actin levels and stimulates growth cone motility. *Neuron* 31:261–275.
- Steward O, Levy WB (1982) Preferential localization of polyribosomes under the base of dendritic spines in granule cells of the dentate gyrus. *J Neurosci* 2:284–291.
- Burgin KE, et al. (1990) In situ hybridization histochemistry of Ca²⁺/calmodulin-dependent protein kinase in developing rat brain. *J Neurosci* 10:1788–1798.
- Colman DR, Kreibich G, Frey AB, Sabatini DD (1982) Synthesis and incorporation of myelin polypeptides into CNS myelin. *J Cell Biol* 95:598–608.
- Martin KC, Ephrussi A (2009) mRNA localization: Gene expression in the spatial dimension. *Cell* 136:719–730.
- Jung H, Gkogkas CG, Sonenberg N, Holt CE (2014) Remote control of gene function by local translation. *Cell* 157:26–40.
- Oberheim NA, et al. (2009) Uniquely hominid features of adult human astrocytes. *J Neurosci* 29:3276–3287.
- Mennerick S, Zorumski CF (1994) Glial contributions to excitatory neurotransmission in cultured hippocampal cells. *Nature* 368:59–62.
- Špaček J (1982) Ribosome-associated membrane contacts between astrocytes in the anoxic brain. *Acta Neuropathol* 57:270–274.
- Doyle JP, et al. (2008) Application of a translational profiling approach for the comparative analysis of CNS cell types. *Cell* 135:749–762.
- Nielsen S, et al. (1997) Specialized membrane domains for water transport in glial cells: High-resolution immunogold cytochemistry of aquaporin-4 in rat brain. *J Neurosci* 17:171–180.
- Dani A, Huang B, Bergan J, Dulac C, Zhuang X (2010) Superresolution imaging of chemical synapses in the brain. *Neuron* 68:843–856.
- Danbolt NC, Storm-Mathisen J, Kanner BI (1992) An [Na⁺ + K⁺]-coupled L-glutamate transporter purified from rat brain is located in glial cell processes. *Neuroscience* 51:295–310.
- Berger UV, DeSilva TM, Chen W, Rosenberg PA (2005) Cellular and subcellular mRNA localization of glutamate transporter isoforms GLT1a and GLT1b in rat brain by in situ hybridization. *J Comp Neurol* 492:78–89.

23. Schmidt EK, Clavarino G, Ceppi M, Pierre P (2009) SUNSET, a nonradioactive method to monitor protein synthesis. *Nat Methods* 6:275–277.
24. Gerstner JR, et al. (2012) Time of day regulates subcellular trafficking, tripartite synaptic localization, and polyadenylation of the astrocytic Fabp7 mRNA. *J Neurosci* 32:1383–1394.
25. Derouiche A, Frotscher M (2001) Peripheral astrocyte processes: Monitoring by selective immunostaining for the actin-binding ERM proteins. *Glia* 36:330–341.
26. Thomsen R, Pallesen J, Daugaard TF, Børjglum AD, Nielsen AL (2013) Genome wide assessment of mRNA in astrocyte protrusions by direct RNA sequencing reveals mRNA localization for the intermediate filament protein nestin. *Glia* 61:1922–1937.
27. Pilaz L-J, Lennox AL, Rouanet JP, Silver DL (2016) Dynamic mRNA transport and local translation in radial glial progenitors of the developing brain. *Curr Biol* 26:3383–3392.
28. Rothstein JD, et al. (1996) Knockout of glutamate transporters reveals a major role for astroglial transport in excitotoxicity and clearance of glutamate. *Neuron* 16:675–686.
29. Chung W-S, et al. (2013) Astrocytes mediate synapse elimination through MEGF10 and MERTK pathways. *Nature* 504:394–400.
30. Kucukdereli H, et al. (2011) Control of excitatory CNS synaptogenesis by astrocyte-secreted proteins Hevin and SPARC. *Proc Natl Acad Sci USA* 108:E440–E449.
31. Christopherson KS, et al. (2005) Thrombospondins are astrocyte-secreted proteins that promote CNS synaptogenesis. *Cell* 120:421–433.
32. Mayford M, Baranes D, Podsypanina K, Kandel ER (1996) The 3'-untranslated region of CaMKII alpha is a cis-acting signal for the localization and translation of mRNA in dendrites. *Proc Natl Acad Sci USA* 93:13250–13255.
33. Andreassi C, Riccio A (2009) To localize or not to localize: mRNA fate is in 3'UTR ends. *Trends Cell Biol* 19:465–474.
34. Condeelis J, Singer RH (2005) How and why does beta-actin mRNA target? *Biol Cell* 97:97–110.
35. Han TW, et al. (2012) Cell-free formation of RNA granules: bound RNAs identify features and components of cellular assemblies. *Cell* 149:768–779.
36. Gruber AR, Lorenz R, Bernhart SH, Neuböck R, Hofacker IL (2008) The Vienna RNA websuite. *Nucleic Acids Res* 36:W70–W74.
37. Halassa MM, Fellin T, Takano H, Dong J-H, Haydon PG (2007) Synaptic islands defined by the territory of a single astrocyte. *J Neurosci* 27:6473–6477.
38. Medvedev N, et al. (2014) Glia selectively approach synapses on thin dendritic spines. *Philos Trans R Soc Lond B Biol Sci* 369:20140047.
39. McLeay RC, Bailey TL (2010) Motif enrichment analysis: A unified framework and an evaluation on ChIP data. *BMC Bioinformatics* 11:165.
40. Galarneau A, Richard S (2005) Target RNA motif and target mRNAs of the Quaking STAR protein. *Nat Struct Mol Biol* 12:691–698.
41. Sidman RL, Dickie MM, Appel SH (1964) Mutant mice (quaking and jimpy) with deficient myelination in the central nervous system. *Science* 144:309–311.
42. Larocque D, et al. (2002) Nuclear retention of MBP mRNAs in the quaking viable mice. *Neuron* 36:815–829.
43. Hardy RJ, et al. (1996) Neural cell type-specific expression of QKI proteins is altered in quaking viable mutant mice. *J Neurosci* 16:7941–7949.
44. Radomska KJ, et al. (2013) RNA-binding protein QKI regulates glial fibrillary acidic protein expression in human astrocytes. *Hum Mol Genet* 22:1373–1382.
45. Greco TM, Seeholzer SH, Mak A, Spruce L, Ischiropoulos H (2010) Quantitative mass spectrometry-based proteomics reveals the dynamic range of primary mouse astrocyte protein secretion. *J Proteome Res* 9:2764–2774.
46. Sharova LV, et al. (2009) Database for mRNA half-life of 19 977 genes obtained by DNA microarray analysis of pluripotent and differentiating mouse embryonic stem cells. *DNA Res* 16:45–58.
47. Lie YS, Macdonald PM (1999) Apontic binds the translational repressor Bruno and is implicated in regulation of oskar mRNA translation. *Development* 126:1129–1138.
48. Huang Y-S, Carson JH, Barbarese E, Richter JD (2003) Facilitation of dendritic mRNA transport by CPEB. *Genes Dev* 17:638–653.
49. Chen KH, Boettiger AN, Moffitt JR, Wang S, Zhuang X (2015) RNA imaging. Spatially resolved, highly multiplexed RNA profiling in single cells. *Science* 348:aaa6090.
50. Sun S, et al. (2015) Translational profiling identifies a cascade of damage initiated in motor neurons and spreading to glia in mutant SOD1-mediated ALS. *Proc Natl Acad Sci USA* 112:E6993–E7002.
51. Rothstein JD, Van Kammen M, Levey AI, Martin LJ, Kundl RW (1995) Selective loss of glial glutamate transporter GLT-1 in amyotrophic lateral sclerosis. *Ann Neurol* 38:73–84.
52. Sun M-Y, Izumi Y, Benz A, Zorumski CF, Mennerick S (2016) Endogenous 24S-hydroxycholesterol modulates NMDAR-mediated function in hippocampal slices. *J Neurophysiol* 115:1263–1272.
53. Bates M, Huang B, Dempsey GT, Zhuang X (2007) Multicolor super-resolution imaging with photo-switchable fluorescent probes. *Science* 317:1749–1753.
54. Reddy AS, et al. (2017) A comprehensive analysis of cell type-specific nuclear RNA from neurons and glia of the brain. *Biol Psychiatry* 81:252–264.
55. Lo HG, et al. (2017) A single transcription factor is sufficient to induce and maintain secretory cell architecture. *Genes Dev* 31:154–171.
56. Westmark PR, Westmark CJ, Jeevananthan A, Malter JS (2011) Preparation of synaptoneuroosomes from mouse cortex using a discontinuous Percoll-sucrose density gradient. *J Vis Exp* 55:3196.
57. Heiman M, et al. (2008) A translational profiling approach for the molecular characterization of CNS cell types. *Cell* 135:738–748.
58. Lorenz R, et al. (2011) ViennaRNA Package 2.0. *Algorithms Mol Biol* 6:26.
59. Bailey TL, Johnson J, Grant CE, Noble WS (2015) The MEME suite. *Nucleic Acids Res* 43:W39–W49.
60. Dougherty JD, et al. (2012) Candidate pathways for promoting differentiation or quiescence of oligodendrocyte progenitor-like cells in glioma. *Cancer Res* 72:4856–4868.
61. Okaty BW, Sugino K, Nelson SB (2011) A quantitative comparison of cell-type-specific microarray gene expression profiling methods in the mouse brain. *PLoS One* 6:e16493.
62. Dougherty JD, Schmidt EF, Nakajima M, Heintz N (2010) Analytical approaches to RNA profiling data for the identification of genes enriched in specific cells. *Nucleic Acids Res* 38:4218–4230.
63. Ike H, et al. (2003) Mechanism of Lck recruitment to the T-cell receptor cluster as studied by single-molecule-fluorescence video imaging. *ChemPhysChem* 4:620–626.
64. Klein RL, King MA, Hamby ME, Meyer EM (2002) Dopaminergic cell loss induced by human A30P alpha-synuclein gene transfer to the rat substantia nigra. *Hum Gene Ther* 13:605–612.
65. Zolotukhin S, et al. (2002) Production and purification of serotype 1, 2, and 5 recombinant adeno-associated viral vectors. *Methods* 28:158–167.
66. Li Z, Zhang Y, Li D, Feng Y (2000) Destabilization and mislocalization of myelin basic protein mRNAs in quaking dysmyelination lacking the QKI RNA-binding proteins. *J Neurosci* 20:4944–4953.
67. Calabretta S, Richard S (2015) Emerging roles of disordered sequences in RNA-binding proteins. *Trends Biochem Sci* 40:662–672.